JOURNAL OF PHYSICAL ORGANIC CHEMISTRY
J. Phys. Org. Chem. 2004; **17:** 439–447
Published online in Wiley InterScience (www.interscience.wiley.com). DOI: 10.1002/poc.751

Electrochemical and theoretical study of a family of fully conjugated dendritic oligomers

Gabriela Osorio,[1] Carlos Frontana,[1] Patricia Guadarrama[2]* and Bernardo A. Frontana-Uribe[1]*

[1]Instituto de Química, UNAM, Circuito Exterior Ciudad Universitaria, Coyoacán, 04510 México D.F., México
[2]Instituto de Investigaciones en Materiales, UNAM, Circuito Exterior s/n, Ciudad Universitaria, Apdo. Postal 70-360, Coyoacán, 04510 México D.F., México

Received 27 October 2003; revised 10 December 2003; accepted 15 December 2003

ABSTRACT: Novel dendritic oligomers of β,β-dibromo-4-ethynylstyrene and formyl-4-ethynylstyrene were electrochemically and theoretically studied in order to gain a better insight into their redox behavior. Correlations between calculated ionization and experimental oxidation potentials (anodic peak potentials) were established. The best correlation was obtained when two important effects are considered in the theoretical calculations, probing their strong influence: (a) structural re-accommodation in the formed radical cation and (b) solvation effects. The effect of dendritic terminal groups (dibromovinyl and formyl groups) was also analyzed. A different redox behavior was observed for these two terminal groups, presumably due to a difference in their oxidation mechanisms. A global chemical transformation for the oxidation of dibromovinyl-terminated oligomers was proposed, providing a satisfactory explanation of the electrochemical behavior within this family of compounds (presence of adsorptive phenomena). Taking these results into account, it is possible to explain how the cation-radical species formed in these conjugated dendritic oligomers behave when cyclic voltammetry technique is applied. Copyright © 2004 John Wiley & Sons, Ltd.

KEYWORDS: dendritic oligomers; cyclic voltammetry; ionization potentials; density functional theory; electrooxidation

INTRODUCTION

There has been increasing interest in hyperbranched and dendritic compounds that incorporate some specific properties in their building blocks, it being possible to have systems capable of showing interesting properties such as the absorption of visible light, carrying out multielectron redox processes or showing luminescent properties in a controlled way.[1] The aforementioned properties could potentially be applied in components for molecular electronics,[2] photochemical molecular devices and information storage.[3] Electroactive dendrimers belong to such a class of compounds with functional groups capable of carrying out fast electron transfer reactions, leading to materials with the mentioned properties. The electroactive groups in dendrimers[4] can be localized at the periphery [e.g. tetrathiafulvalene (TTF) units[5] or electroactive ferrocene subunits at the periphery[6]] or in the interior (an example is the reported dendrimers using porphyrin cores[7]).

**Correspondence to:* P. Guadarrama and B. A. Frontanta-Uribe, Instituto de Investigaciones en Materiales, UNAM, Circuito Exterior s/n, Ciudad Universitaria, Apdo. Postal 70-360, Coyoacán, 04510 México D.F., México and Instituto de Química, UNAM, Circuito Exterior Ciudad Universitaria, Coyoacán, 04510 México D.F., México.
E-mail: patriciagua@correo.unam.mx
Contract/grant sponsor: CONACYT; *Contract/grant numbers:* J34873-E and 137005U.

Recently, the synthesis of well-defined conjugated dendritic oligomers of β,β-dibromo-4-ethynylstyrene was carried out[8] (see Fig. 1). Discrete, conjugated units were included, resulting in a family of blue emitters with an emission range of 440–500 nm. According to the classification mentioned above, these oligomers belong to the group of dendrimers having internal electroactive groups. The study of the electrochemical behavior of these compounds is presented as an interesting issue, considering their high electron delocalization.

Among the electrochemical techniques, cyclic voltammetry (CV) has gained considerable popularity since it provides a quick and fairly straightforward assessment of the redox behavior of molecular systems, which parallels that of spectrophotometric techniques for luminescent properties.[9] Several important parameters of CV, such as peak potential (energetic parameter of formation of species) and current function values ($I_p v^{-1/2} C^{-1}$), provide useful information needed to obtain both coupled processes and stoichiometry of the electrochemical reactions.[10] In the case of macromolecular systems, it is known that electrochemical data offer unequivocal information on the chemical and topological structure involved. Therefore, it was decided to apply this technique in combination with theoretical calculations in order to study the dendritic oligomers **I–IV**, seeking to establish

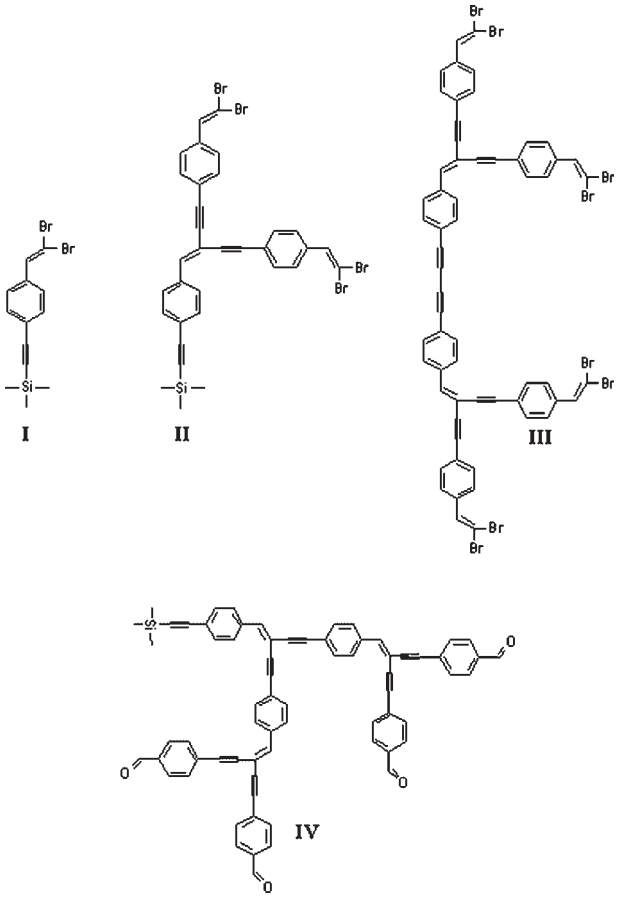

Figure 1. Dendritic oligomers with ethynylstyryl conjugated units

structure–property relationships, useful for the future design of novel materials.

In the present study, CV parameters of the fully conjugated dendritic oligomers **I–IV** were analyzed and compared with theoretical results. A previous report gave ionization potential theoretical data for these kinds of dendritic oligomers in the gas phase.[11] Here were carried out theoretical calculations considering the solvation effect and the structural relaxation effect (adiabatic conditions) after the oxidation process. Very good correlations were obtained with the experiment when such effects are involved.

EXPERIMENTAL

Compounds **I–IV** (Fig. 1) were previously synthesized and fully characterized.[8] The electrolytic media consisted of a 3:1 mixture of anhydrous acetonitrile (Aldrich) and dichloromethane (previously dried with CaH_2), using as support electrolyte 0.1 M tetrabutylammonium perchlorate (TBAP) (dried at 80 °C overnight). A conventional three-electrode cell was used for the electrochemical experiments, employing a platinum, nickel microelectrode (BAS, surface area 0.033 cm^2) and vitreous carbon microelectrode (BAS, surface area 0.06 cm^2) as working electrodes. A platinum mesh was used as counter electrode (surface area 0.66 cm^2). The values of potential were obtained against the pseudo-reference of Ag/0.01 M $AgNO_3$, 0.1 M TBAP in acetonitrile (BAS), separated from the medium by a Vycor membrane. The potentials reported in this work are referred to the ferricinium/ferrocene couple (Fc^+/Fc), according to the IUPAC recommendation.[12] The potential of the Fc^+/Fc couple against this reference electrode was 0.25 V. The solution was deoxygenated for 15 min and the cell was kept under a nitrogen atmosphere (grade 5, Praxair) throughout the voltammetric experiments. CV was performed with an Autolab PGSTAT 30 potentiostat/galvanostat, and data were analyzed using GPES software version 4.9 available from the manufacturer. *IR* drop correction was applied after data acquisition in order to evaluate the kinetic functions.

THORETICAL METHODOLOGY

All calculations of ionization potentials considering the solvation effects and adiabatic conditions were performed using Jaguar version 4.2, release 73.[13] Initial geometries were generated by Chem3D and optimized using PM3. Solvation energies were obtained at the B3LYP/6–311** level of theory, using a LACVP* basis set for bromine atoms. A continuum dielectric constant of 38 and a solvent probe molecule radius of 2.18 Å were considered for acetonitrile. The interactions between the molecules and the solvent were evaluated by Jaguar's Poisson–Boltzmann solver, in which the field produced by the solvent dielectric continuum was fitted to the solvent point charges. These solvent point charges are fed backed into the SCF (self-consistent-field), which performs a new calculation of the wavefunction for the molecules in the field produced by the solvent. Adiabatic ionization potentials in the gas phase were computed using Gaussian 98.[14] After geometry optimization with PM3, single point calculations were carried out at the B3LYP/3–21G(d) level of theory. Frequency calculations including thermochemical analysis were carried out at the B3LYP/LACVP** level of theory in order to obtain Gibbs free energy data (G_{TOT}) at standard temperature and pressure, for molecules **A**, **B**, **C**, **D** and **E** (see Figure 11).

Atomic charges were derived from the electrostatic potential computation. The electrostatic potential is calculated creating an electrostatic potential grid. The point charges are derived from such a grid.

RESULTS AND DISCUSSION

In the CV experiments, it could be observed that the shape of the voltammograms was dependent on the terminal groups present in the analyzed oligomers (Fig. 2).

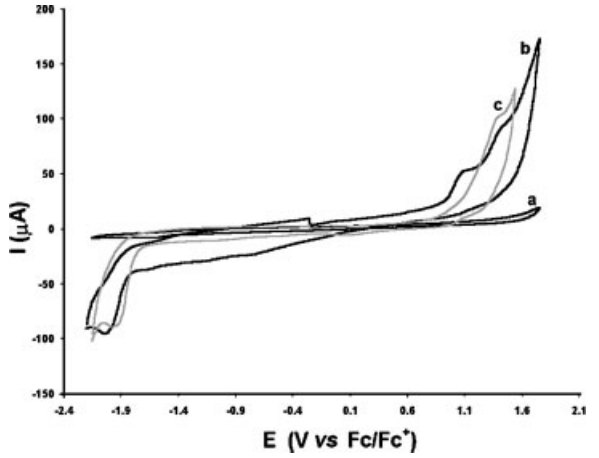

Figure 2. Typical cyclic voltammogram of oligomers **II** and **IV** (0.7 mM), obtained with a platinum microelectrode (0.033 cm^2) in 0.1 M TBAP in acetonitrile–dichloromethane (3:1). The potential scan was initiated from -0.25 V vs Fc/Fc^+ towards the positive direction (100 mV s^{-1}). (a) Electroanalysis medium; (b) oligomer **II** present; (c) oligomer **IV** present

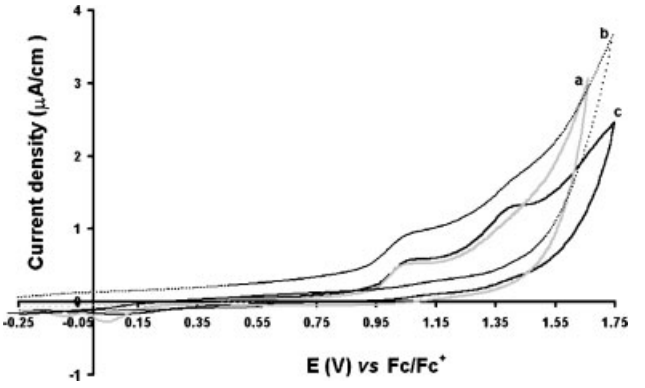

Figure 3. Voltammetric response with different electrode materials of the anodic region for oligomer **II** (0.7 mM) in 0.1 M TBAP in acetonitrile–dichloromethane (3:1). The potential scan was initiated from -0.25 V vs Fc/Fc^+ towards the positive direction (100 mV s^{-1}). (a) Nickel electrode (0.033 cm^2); (b) Vitreous carbon electrode (0.066 cm^2); (c) platinum electrode (0.033 cm^2)

Compound **IV**, with terminal formyl groups, showed a completely different behavior to the other oligomers, screening a single irreversible oxidation signal. On the other hand, the family of compounds (**I–III**) with dibromovinyl terminal groups showed two irreversible oxidation signals. In the cathodic region, two very close irreversible signals were found for all compounds showing no association with the anodic signals. This behavior was observed over the entire range of scan rates studied (up to 2 V s^{-1}) and was confirmed by a study of the inversion potential scan towards the positive direction ($E_{\lambda+}$). Electrochemical data for the studied compounds are presented in Table 1.

The difference in redox behavior depending on the terminal groups, containing the same conjugated backbone, demonstrates that those groups determine the direction of oxidation processes, following different mechanisms. In order to make a systematic correlation between electrochemical data from the same redox processes with the accurate theoretical data, the formyl oligomer **IV** was excluded from the subsequent electrochemical analysis. This criterion was also applied to the theoretical study and will be discussed later.

Therefore, with the aim of understanding the redox behavior of the dibromovinyl-terminated oligomer family **I–III**, a deeper voltammetric study of the anodic reactions for a model compound of the family (**II**) was carried out. The shape of the observed signals for this oligomer shows a strong dependence on the electrode material used (platinum, vitreous carbon and nickel, Fig. 3). This result represents a qualitative test of an inner-sphere redox mechanism[15] where adsorption–desorption processes are very important. It can also be observed that by using platinum surfaces, a well-defined voltammogram can be obtained, so the analysis was continued with this electrode material. The electrode was gently polished with an absorbent paper and acetone to acquire reproducible signals. The small cathodic signal at 0.1 V was assigned to the reduction of the medium, probably from the residual water.

An important decrease in the current signal was clearly observed when consecutive cyclic voltammograms of the anodic region were carried out (Fig. 4). Another important feature of the curves was their shape when the potential scan was reversed. A fast decay without the classical diffusion shoulder in the wave was observed, this result being a qualitative indication of an irreversible adsorption process.[16] These observations indicate the presence of an important adsorption process mixed with the electron transfer that diminishes the electroactive surface of the electrode.

Table 1. Electrochemical data for dendritic oligomers **I–IV**[a]

Oligomer	E_{pIA}(V vs Fc/Fc^+)	E_{pIIA}(V vs Fc/Fc^+)	E_{pIc}(V vs Fc/Fc^+)[b]
I	1.01	1.425	−2.203
II	1.003	1.325	−1.929
III	1.015	1.296	−2.023
IV	—	1.190	−1.992

[a] Obtained from the CV experiments (100 m V s^{-1}) carried out in anhydrous acetonitrile–dichloromethane (3:1). TBAP, 0.1 M·E_{Ref}, Ag/Ag^+; E_{Aux}, Pt; E_{wk}, Pt.
[b] The second cathodic peak is observed as a shoulder.

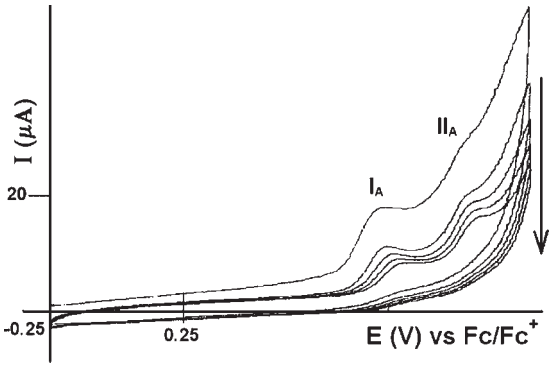

Figure 4. Five consecutive cyclic voltammograms of the anodic region of oligomer **II** (0.7 mM) obtained with a platinum microelectrode (0.033 cm^2) in 0.1 M TBAP in acetonitrile–dichloromethane (3:1). The potential scan was initiated from -0.25 V vs Fc/Fc^+ towards the positive direction (100 mV s^{-1})

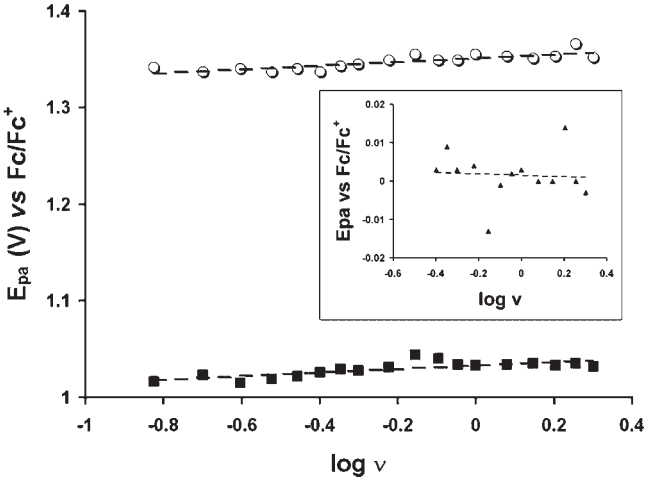

Figure 5. Variation of the potential of the oxidation peaks of 0.7 mM oligomer **II** with logarithm of the scan rate potential: (■) peak IA; (○) peak IIA; (▲) Fc 0.7 mM at the onset. Slope values for the indicated regions are 19, 20 and 2 mV per decade, respectively

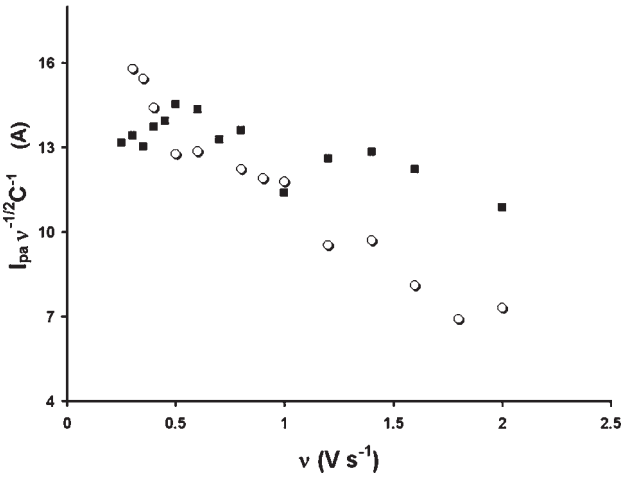

Figure 6. Variation of the voltammetric current function ($I_{pa}\nu^{-1/2}C^{-1}$) with scan rate potential (V s^{-1}) for both peaks of oligomer **II**: (■) peak I_A; (○) peak II_A

The analysis of the peak potential (E_{pa}) versus the logarithm of the scan rate (Fig. 5) for peaks I_A and II_A for oligomer **II** shows that the E_{pa} values shift anodically for both signals, with slopes of $\sim$20 mV per decade each (2.0 mV per decade for the ferrocene/ferricinium couple). This behavior indicates that the ratio between the relative amounts of oxidized and reduced species at the electrode surface increases with the scan rate. This means that, at higher scan rates, the electrochemical reaction sequence approaches a mechanism with lower stoichiometry, as reported for an EC process (chemical reaction following the electronic transfer).[17] It is known from literature that the slope value is dependent on the ratio of the homogeneous and heterogeneous constants, and comparison with the theoretical ideal value (30 mV/n for a 10-fold increase in ν for a fast electron transfer coupled with a fast chemical reaction) is difficult because these conditions were not confirmed in our case and the adsorption process could complicate the overall mechanism, affecting the slope value. Even so, the tendency of the curve clearly indicates a coupled reaction with the electron transfer.

The study of the current function ($I_{pa}\nu^{-1/2}C^{-1}$) for peaks I_A and II_A showed different behavior with the scan rate (Fig. 6). For peak I_A, the function increases for scan rates up to 0.6 V s^{-1} and then decreases. For the second anodic peak, II_A, this function decreases over the entire scan rate range. The linear increment on the current function values for peak I_A is characteristic of an adsorption reaction[18] and it could be associated with the chemical composition of the molecule (presence of silicon on the backbone of the structures) or its high electron delocalization, as has been reported previously for electrode preparation.[19] This adsorption process is present in all the tested electrode materials for all the oligomers, leading to partial or total passivation of the surface, affecting the presence of peak II_A. Particularly for **IV** in all the materials, after the first cycle in the CV experiment, it was impossible to observe the oxidation signal again. The fact that the adsorption peak appears before the Faradaic process has been reported to be associated with strong adsorption of the electron transfer product.[18] The change in the relative intensities *vis-a-vis* the peak II_A when the concentration of electroactive species was increased, reinforced the proposal of an adsorption process as an explanation for peak I_A.

The behavior of the current function for peak II_A can be associated with a mechanism of type EC. This mechanism shows, at low scan rates, higher currents owing to a decrease in the relative stoichiometry in the transformation sequence.[20]

Table 2. Adiabatic and vertical calculated ionization potentials, total energies and frontier orbital HOMO energies

Molecule	IP_a (eV) (gas phase)	IP_a[a] (eV) (solution phase)	IP_v (eV)	IP (eV) (Koopman)	E_T (Ha) (solution phase)	E_{HOMO} (Ha) (solution phase)
I	7.25	5.68	7.66	8.46	−819.56	−0.227
$\mathbf{I}^{+\cdot}$					−819.35	
II	6.27	5.07	6.72	7.66	−1614.28	−0.213
$\mathbf{II}^{+\cdot}$					−1613.67	
III	5.67	4.85	5.94	5.44	−2409.17	−0.200
$\mathbf{III}^{+\cdot}$					−2408.99	
IV	6.02	5.05	6.57	8.99	−3245.82	−0.203
$\mathbf{IV}^{+\cdot}$					−3245.63	

[a] Solvation energies were obtained at the B3LYP/6–311** level of theory, using the LACVP* basis set for bromine atoms (geometries were obtained at the PM3 level).

With these experimental data for the oxidation peak II_A, the following mechanistic route is proposed for this family of oligomers:

$$A - e^- \rightarrow B^{+\cdot}$$
$$B^{+\cdot} \rightarrow C$$
$$C \rightarrow C\ (ads)$$

From a theoretical point of view, some calculation using quantum mechanics methods were carried out with the aim of describing the electronic behavior of these systems in the presence of a solvent. One of the issues to analyze is the fact that, as stated before, terminal groups (—HC═CBr_2 and —CHO) showed a different behavior in the oxidation processes. There are several factors that affect the oxidation processes and some information can be obtained from the ionization potential values and from the charge distribution. According to previous calculations,[11] the general tendency showed that ionization potentials, both vertical and adiabatic, are higher for oligomers with formyl terminal groups in comparison with those with dibromovinyl terminal groups, for the same dendritic generation. This was attributed to the high polarizability of bromine atoms facilitating the electron subtraction. Considering now the acetonitrile solvent (see Theoretical methodology), the same theoretical behavior can be observed (Table 2). It is noticeable that adiabatic ionization potentials are always lower than vertical ionization potentials and such a difference in energy should come from the molecular geometry relaxation and subsequent electronic redistribution after the ionization in an adiabatic process.

The experimentally observed differences in the electrochemical behavior of molecules bearing dibromovinyl or formyl terminal groups was also confirmed theoretically by the correlation between oxidation electrode potentials and ionization potentials. Several of these correlations have been reported previously for other systems.[21] When the correlation between oxidation potentials and calculated ionization potentials was carried out, in both the gaseous and solution phases, the expected linear tendency was not observed when molecule **IV** (with formyl terminal groups, open square) is included. Figure 7 clearly illustrates this fact in the solution phase.

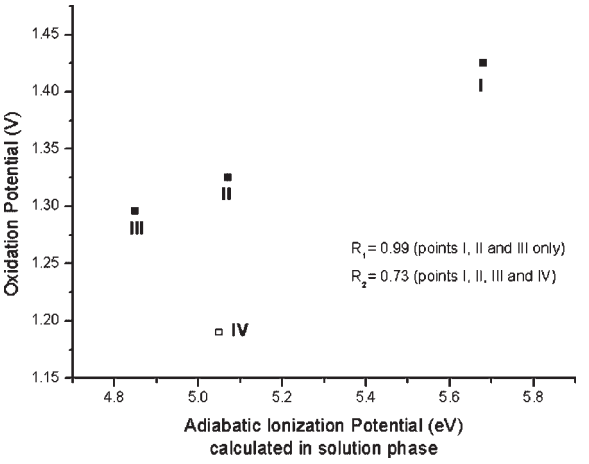

Figure 7. Experimental oxidation potentials vs. IP_a (adiabatic ionization potentials) in the solution phase (calculated at the B3LYP/6–311** level of theory)

Once the same family of molecules is considered (**I**–**III**), it is possible to obtain a very good correlation between experimental and theoretical data when two factors are included in the calculations: first, the consideration of adiabatic conditions leading to the reaccommodation of molecular structures after an oxidation process, and second, the solvation effect, involving acetonitrile as solvent. The closed squares in Fig. 7 show the good linear fitting ($R = 0.99$) for molecules **I**, **II** and **III**. This result is indicative that the solvent interactions play an important role in the ionization processes. The same correlation but in the absence of solvent resulted in a worse linear fitting.

A schematic picture of resonant structures for the cation-radical precursor of the first dendritic generation with formyl terminal groups was proposed (Fig. 8). The formation of an acyl radical is feasible[22] and can explain the Faradaic oxidation process. This radical can react with the solvent, as has been reported for carbon center radicals in the presence of nitrile functions to give neutral species.[23]

A similar schematic representation is presented for cero-dendritic generation with the dibromovinyl terminal

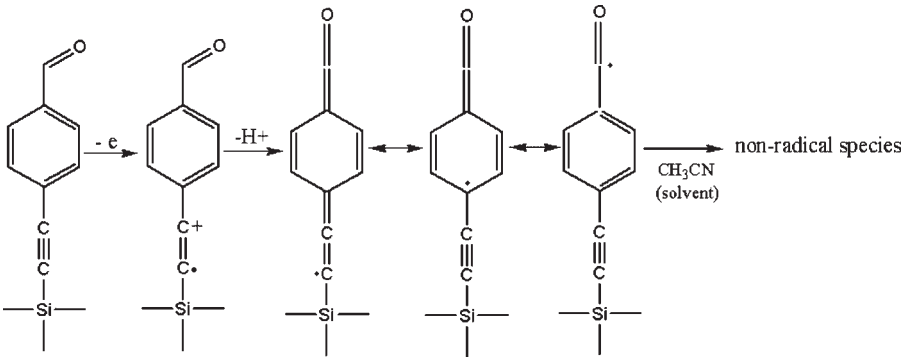

Figure 8. Resonant structures for cation-radical oligomer with formyl terminal groups

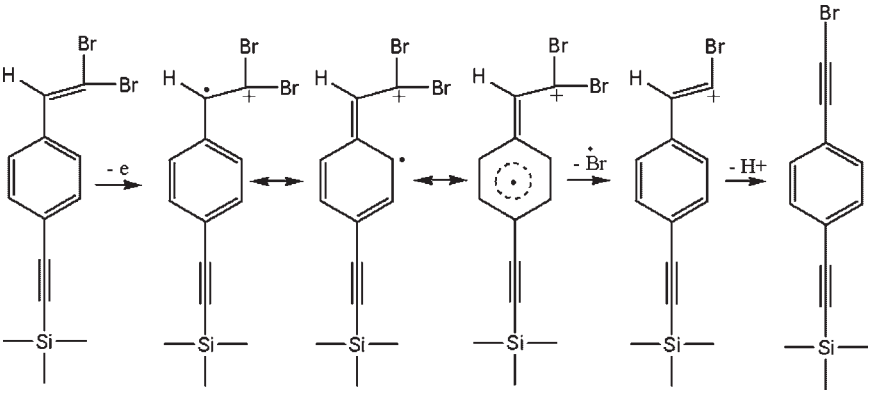

Figure 9. Resonant structures for cation-radical oligomer with dibromovinyl terminal groups

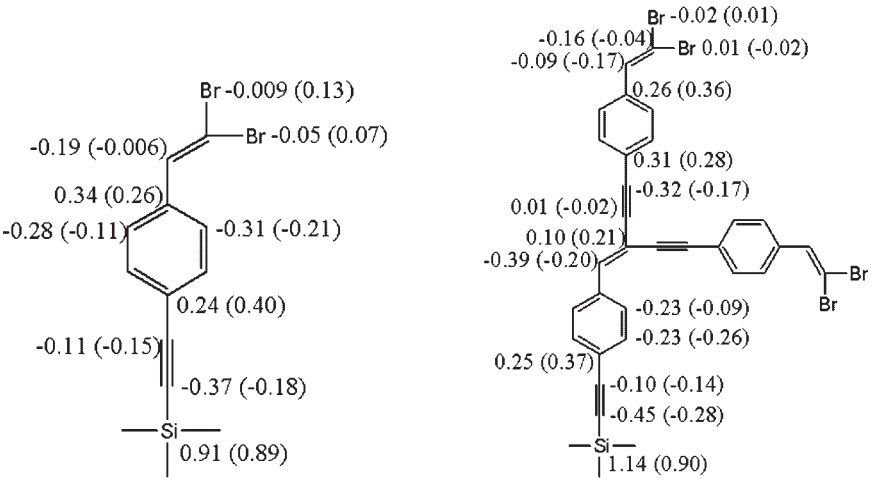

I **II**

Figure 10. Atomic charges from electrostatic potential for molecules **I** and **II**. In parentheses are the values corresponding to cation-radical species

group, describing the possible mechanism for the stabilization of the oxidized species (Fig. 9). Atomic charges calculated from the electrostatic potential are in agreement with the proposed chemical route. Charges corresponding to neutral and cation-radical species (values in parentheses, Fig. 10) show that the vinylic group is involved in the formation of the cation-radical, considering its participation in terms of the charge difference between neutral and cation-radical species; however, once this cation-radical is formed, the delocalization takes place as shown in the scheme. On the other hand, the low negative density charge on bromine terminal atoms, in combination with their inherent polarizability, turns them into feasible leaving groups as radical species. In this way, bromine

atoms participate in the stabilization of positive charge in the oxidation process, allowing the possible formation of the bromoethynyl moiety attached to the benzene ring (final structure in Fig. 9).

There are some chemical criteria to be mentioned in order to support the proposed mechanism over other possible chemical processes such as polymerization or even some kind of cyclizations. The reason why a new mechanism is being proposed is because experimentally it was observed that, depending on the terminal dendritic group, formyl or dibromovinyl, a different electrochemical behavior is found. In molecule **I**, if any polymerization process is taking place, the disubstituted styryl moiety will not be participating, considering its low reactivity towards polymerization (either radical or cationic) due to steric hindrance. It is known that, in terms of reactivity, to facilitate polymerization reactions, the maximum number of substituents at a styrenic carbon–carbon double bond is one per carbon atom, that is, PhCHX═CHX, otherwise polymerization reactions are not observed. This was reconfirmed by evaluating the formation of a dimer from two molecules of compound **I** by calculations of Gibbs free energy values at the B3LYP/LACVP* level of theory, resulting in an unfavorable process [$\Delta G = 85.3\,\text{kcal mol})^{-1}$ ($1\,\text{kcal} = 4.184\,\text{kJ}$)].

The other possible active site to initiate a polymerization process is the ethynyl group. Such an ethynyl group is also present in the dendritic oligomers with formyl-terminal groups, such as **IV**, and no experimental evidence of polymerization processes was observed at all in that case. Another important argument against the polymerization reactions is the low concentration used to carry out the electrochemical experiments ($1.25 \times 10^{-6}\,\text{mol cm}^{-3}$). On the other hand, cyclization reactions appear very improbable owing to the high rigidity found in this aromatic dendritic oligomers.

Experimentally, the differences discussed so far between molecules **I**, **II** and **III** and molecule **IV** are presumably due to the presence of an adsorptive process when dibromovinyl terminal groups are present.

Considering the electrochemical medium, specifically acetonitrile as a solvent, a chemical reaction describing the transformation of molecule **I** is proposed as shown in Fig. 11, leading to the formation of monobromine molecule **C**. Frequency calculations including thermochemical analysis were carried out at the B3LYP/LACVP** level of theory in order to obtain Gibbs free energy data (G_{TOT}) at standard temperature and pressure for molecules **A**, **B**, **C**, **D** and **E**.

According to the energetic criteria, the formation of the monobromine molecule **C**, accompanied by the formation of the protonated form of acetonitrile (**D**) and a bromo radical (**E**), provides the driving force for the process to occur. Reasonable negative Gibbs free energy for this process is achieved ($\Delta G = -47.46\,\text{kcal mol}^{-1}$) when this mechanism is considered. The formation of small species, such as **D** and **E**, in the scheme also favors the proposed chemical reaction in terms of the enthalpic and entropic contributions.

Molecule **C** is presumably the most likely species to be adsorbed on the electrode surface. It has been reported that π-electron-rich organic molecules are more easily adsorbed than other organic molecules over metallic electrodes.[24] This has been explained by the favored overlap of the d orbitals of the electrode transition metals with the π-electrons of the organic molecules. This property has also been observed in other surfaces such as highly oriented pyrolytic graphite (HOPG), where the aromatic groups are always adsorbed parallel to the surface, as observed in atomic force microscopic visualizations of isophthalic and terephthalic acid derivative monolayers.[25] Thus, molecule **C**, owing to the presence

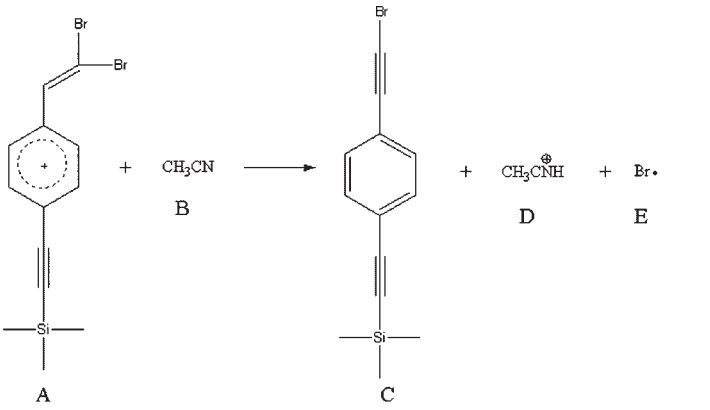

Figure 11. Oxidation reaction proposed for **II**. Gibbs free energies calculated at the B3LYP/LACVP** level of theory in the solution phase at standard temperature and pressure

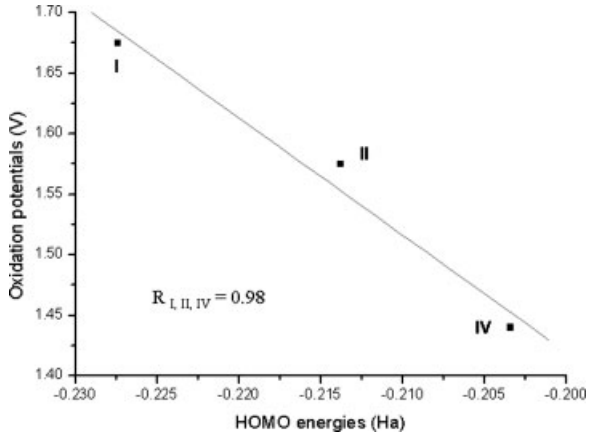

Figure 12. HOMO energies in the solution phase vs experimental oxidation potentials for molecules **I**, **II** and **IV**

of the π-electron system and also the presence of polarizable bromine atoms, in addition to the planar shape adopted, becomes suitable to undergo adsorption on the electrode surface.

To complete the description of these systems, total energies were calculated within the density functional theory (DFT). Table 2 gives the total energies and frontier orbital energies, all of them calculated in solution. The total energy values are in agreement with the growth in the size of delocalized systems from molecule **I** to molecule **IV**, being more negative for those molecules with major conjugation. This trend is retained in the case of cation-radical molecules.

With respect to frontier orbitals, there is a known correlation between the molecular orbital HOMO energy and oxidation potentials. Less positive oxidation potentials are to be expected for compounds with higher HOMO energies. The energy and shape of the HOMOs depend on the electron density distribution in the molecules. In the specific case of highly delocalized molecules, the extension of the π-systems is directly related to the energetic level of such orbitals. According to this, the calculated HOMO energies in solution phase of **I**, **II** and **IV**, all with the same delocalized backbone pattern, were correlated with their oxidation potentials obtained experimentally, showing a good linear correlation (see Fig. 12). This result again confirms that the electroactive compounds are the monomeric species, since the HOMO energies for extended delocalized polymeric structures should be very different, and no correlation with monomeric compound **IV** could be possible.

It is noticeable that, even when the intrinsic limitations of the theoretical models are actually present, the correlation observed between the experiment and calculations is acceptable. Thus, the use of CV in conjunction with theoretical calculations provided interesting insights into the behavior of dendritic oligomers with ethynylstyryl discrete conjugated units and different terminal groups.

CONCLUSIONS

A series of conjugated dendritic oligomers (**I–IV**) was studied by the CV and theoretical calculations were carried out in order to propose an explanation of the irreversible behavior observed experimentally for these compounds. In CV, two oxidation signals were observed for the family of compounds **I–III** (bearing dibromovinyl terminal groups), one of them being attributed presumably to a specific adsorption on the electrode surface *via* coupled chemical phenomena after the electron transfer (EC reaction).

Considering the voltammetric results for dibromovinyl-terminated dendritic oligomers, a global chemical transformation was proposed and thermochemical data for total Gibbs energies were calculated in order to support such a transformation scheme (Fig. 11). These calculations, in combination with some other good correlations between experimental and theoretical data make the scheme reliable. The value of the Gibbs free energy obtained by frequency calculations at the B3LYP/LACVP** level of theory was $\Delta G = -47.46\,\text{kcal mol}^{-1}$, which energetically supports the formation of molecule **C** in addition to the formation of small species **D** and **E**, which contribute in terms of enthalpy and entropy. Hence, molecule **C** was suggested to be the one adsorbed on the electrode surface.

All the results obtained demonstrate that CV is a convenient technique for the study of dendritic systems. Furthermore, these experimental results validate the theoretical methods used.

The correlations between experimental and theoretical data indicate that both the re-accommodation (adiabatic conditions) and solvation factors are very important and should be considered in the theoretical models since there is a better coincidence between theory and experiments when they are included. Such a coincidence between experiments and the computational methods used in the present study leaves a door open for further multidisciplinary work.

Acknowledgements

The authors are indebted to Gabriela Salcedo for language correction and Dr Sergei Fomine for helpful comments. This work was partially supported by CONACYT grants J 34873-E and 137005U. This is contribution number 2468 from IQ UNAM.

REFERENCES

1. (a) Jiang DL, Aida TM. *J. Am. Chem. Soc.* 1998; **120**: 10895–10901; (b) Bao Z, Amundson KR, Lovinger AJ. *Macromolecules* 1998; **31**: 8647–8649; (c) Malenfant PRL, Groenendaal L, Frechet JMJ. *J. Am. Chem. Soc.* 1998; **120**: 10990–10991.

2. Miller L, Duan R, Tully D, Tomalia D. *J. Am. Chem. Soc.* 1997; **119**: 1005–1010.
3. Tomiok N, Takasu D, Takashi D, Aida T. *Angew. Chem., Int. Ed. Engl.* 1998; **37**: 1531–1534.
4. Kaifer A, Gómez-Kaifer M. *Supramolecular Electrochemistry.* Wiley-VCH: New York, 1999.
5. Bryce MR, Devonport W, Moore AJ. *Angew. Chem., Int. Ed. Engl.* 1994; **33**: 1761–1763.
6. Alonso B, Morán M, Casado CM, Lobete F, Losada J, Cuadrado I. *Chem. Mater.* 1995; **7**: 1440–1442.
7. (a) Dandliker PJ, Diederich F, Gross M, Knobler CB, Louati A, Sanford EM. *Angew. Chem., Int. Ed. Engl.* 1994; **33**: 1739–1742; (b) Dandliker PJ, Diederich F, Zingg A, Gisselbrecht JP, Gross M, Louati A, Sanford EM. *Helv. Chim. Acta* 1997; **80**: 1773–1801.
8. Fomina L, Guadarrama P, Fomine S, Salcedo R, Ogawa T. *Polymer* 1998; **39**: 2629–2635.
9. Heinze J. *Angew. Chem., Int. Ed. Engl.* 1984; **23**: 831–847.
10. (a) Gosser DK. *Cyclic Voltammetry: Simulation and Analysis of Reaction Mechanisms.* Wiley-VCH: New York, 1993; 71–102; (b) Brown ER, Sandifer JR. In *Physical Methods of Chemistry*, Rossiter BW, Hamilton JF (eds). Wiley: New York, 1986; 273–345.
11. Fomine S, Fomina L, Guadarrama P. *J. Mol. Struct.* 1999; **488**: 207–216.
12. Gritzner G, Küta J. *Pure Appl. Chem.* 1984; **4**: 462–466.
13. *Jaguar 4.2*. Schrodinger: Portland, OR, 2000.
14. Frisch MJ, Trucks GW, Schlegel HB, Scuseria GE, Robb MA, Cheeseman JR, Zakrzewski VG, Montgomery JA Jr, Stratmann RE, Burant JC, Dapprich S, Millam JM, Daniels AD, Kudin KN, Strain MC, Farkas O, Tomasi J, Barone V, Cossi M, Cammi R, Mennucci B, Pomelli C, Adamo C, Clifford S, Ochterski J, Petersson GA, Ayala PY, Cui Q, Morokuma K, Malick DK, Rabuck AD, Raghavachari K, Foresman JB, Cioslowski J, Ortiz JV, Baboul AG, Stefanov BB, Liu G, Liashenko A, Piskorz P, Komaromi I, Gomperts R, Martin RL, Fox DJ, Keith T, Al-Laham MA, Peng CY, Nanayakkara A, Challacombe M, Gill PMW, Johnson B, Chen W, Wong MW, Andres JL, Gonzalez C, Head-Gordon M, Replogle ES, Pople JA. *Gaussian 98, Revision A.9*. Gaussian: Pittsburgh, PA, 1998.
15. Torres LM, Gil AF, Galicia L, González I. *J. Chem. Educ.* 1996; **73**: 808–812.
16. Bard AJ, Faulkner LR. *Electrochemical Methods* (2nd edn). Wiley: New York, 2001; 600–601.
17. Savéant JM, Vianello E. *Electrochim. Acta* 1967; **12**: 629–646.
18. Brown ER, Sandifer JR. In *Physical Methods of Chemistry*, Rossiter BW, Hamilton JF (eds). Wiley: New York, 1986; 336–341.
19. Murray RW. *Molecular Design of Electrode Surfaces.* Wiley–Interscience: New York, 1992.
20. Brown ER, Sandifer JR. In *Physical Methods of Chemistry*, Rossiter BW, Hamilton JF (eds). Wiley: New York, 1986; 333–334.
21. (a) Parker V. *J. Am. Chem. Soc.* 1976; **98**: 98–103; (b) Neikam WC, Dimeler GR, Desmond MM. *J. Electrochem. Soc.* 1964; **111**: 1190; (c) Pysh ES, Yang NC. *J. Am. Chem. Soc.* 1963; **85**: 2124–2130.
22. Chatgilialoglu C, Crich D, Komatsu M, Ryu I. *Chem. Rev.* 1999; **99**: 1991–2070.
23. Fossey J, Lefort D. *Les Radicaux Libres en Chimie Organique.* Masson: Paris, 1993; Chapt. 13, 168.
24. Kiselev VF, Kylov O. *Adsorption and Catalysis on Transition Metals and Their Oxides.* Springer: New York, 1989; 164–169.
25. De Feyter S, Gesquière A, Abdel-Mottaleb MM, Grim PCM, De Scheyver FC, Meiners C, Sieffert M, Valiyaveettil S, Müllen K. *Acc. Chem. Res.* 2000; **33**: 520–531.